Beam Steering Characteristics of Reconfigurable Transmitarray Antennas

Subjects: Engineering, Electrical & Electronic

Contributor: Qasim Ali

The high gain beam steering antennas are widely used in 5G wireless mobile communications, radio frequency (RF) wireless power transmission, and satellite communications. In order to obtain high gain and beam steering characteristics, traditionally, antennas of the same type as phased array antennas, reflectarray antennas, and parabolic antennas have been designed. The transmitarray (TA) has attracted more and more interest from researchers due to its low profile, affordable cost, lower losses, low design complexity, and ease of fabrication. These have become popular solutions due to their remarkable applications, for instance, in biomedical systems (Brain and Breast Cancer Detection), civil and military radar systems, imaging systems, satellite communications, direct broadcasting services, and 6G/5G communication systems, etc.

reconfigurable transmitarray | beam steering | beamforming | PIN diodes | varactor | MEMS | dual-band transmitarray | multi-bit transmitarray

1. Introduction

The high gain beam steering antennas are widely used in 5G wireless mobile communications, radio frequency (RF) wireless power transmission, and satellite communications [1][2][3]. In order to obtain high gain and beam steering characteristics, traditionally, antennas of the same type as phased array antennas, reflectarray antennas, and parabolic antennas have been designed [4][5][6]. However, these types of antennas have some disadvantages despite their excellent characteristics since the parabolic antenna and the dielectric lens antenna have a curved shape (i.e., non-planar structures), are expensive, and difficult to manufacture. In addition, a planar phased array antenna with high gain characteristics in the millimeter-wave band may have a complex feeding structure with losses that might influence the antenna's overall radio performance.

Transmitarrays also considered as lens arrays or lenses were first presented in [7] by achieving control on EM waves. A lens antenna was proposed in [8] with a characteristic change that can control the wavefront of transmitted and reflected electromagnetic waves. Using a simple microwave lens antenna to attach two patch antennas with a center probe to transfer electromagnetic (EM) energy, the configuration was able to perform characteristics of scanning and focusing of an EM beam by microwave lens antenna. Microwave lenses obtained more interest when researchers achieved a better understanding of planar antennas and microstrip patch antennas [9]. Transmitarray uses a simple Snell's law for working operation, which causes a narrow bandwidth and time-consuming structures. All dielectric and all metal structures are adopted to improve their capabilities for these

disadvantages. All dielectric structures are widely utilized for transmitarrays due to their high transmittance, low cost, easy fabrication, and lightweight qualities [10][11][12]. TA structures develop with all dielectric materials, while a genetic algorithm (GA) and practical swarm optimization algorithm (PSO) are applied to optimize each pillar unit cell [13][14]. The integrated optimization strategy increases design reliability while freeing up human effort and time. Furthermore, in order to achieve wideband characteristics, the optimizing goal is to design a rectangular area to accommodate the source antenna's shifting phase center. As researchers develop all dielectric TA designs, 3D printing technology can easily fabricate designs and provides advantages of being lightweight, low cost, and easy to fabricate.

All dielectric TAs have some disadvantages as compared to all metal TAs such as high profile, low machining accuracy, and electromagnetic properties of high power microwave applications [15]. Furthermore, for some applications, TAs are utilized in harsh working environments such as space. In these conditions, TAs without dielectric materials adapt to environmental conditions better than dielectric materials and reduce fabrication cost. Dielectric materials are not appropriate for high frequencies, whereas metals have low-frequency electromagnetic effects on high frequencies. Many studies have been proposed in the literature for all metal transmitarrays [16][17][18][19]. Most of them adopt the multilayer method to obtain 360 degrees phase shift and low losses amplitude. Many improvements deliver for all metal TAs but their bandwidth is still relatively low.

The transmitarray (TA) has attracted more and more interest from researchers due to its low profile, affordable cost, lower losses, low design complexity, and ease of fabrication. These have become popular solutions due to their remarkable applications, for instance, in biomedical systems (Brain and Breast Cancer Detection), civil and military radar systems, imaging systems, satellite communications, direct broadcasting services, and 6G/5G communication systems, etc. [20][21][22][23][24][25][26]. Transmitarrays (TAs) are primarily composed of several discrete unitary elements, and special feed sources (horn antenna, microstrip patch antennas, or other UWB antennas) are used to illuminate EM waves. They also used multilayer frequency selective surfaces, meta-materials, and metasurfaces [27][28][29]. There are various dynamic technologies exploited to enable the reconfigurable characteristics of TAs. Reconfigurable features perform electronic beam forming or beam steering, frequency tuning, and the control of polarization by solid-state electronics devices such as using PIN diodes [30][31][32], varactors [33], MEMS (micro-electromechanical systems) switches [34], tunable dielectric substance liquid crystals [35][36], microfluidic systems [37], and graphene [38]. All these components have dynamic performance with respect to their advantages and disadvantages; PIN diodes and varactors are commonly used in solid-state devices available for lower radio frequencies up to 40 GHz [39][40]. In recent years, substantial advancements have been made in the development and implementation of reconfigurable technology for antennas and other solid-state devices.

Versatile communication systems and radars have upsurged the demand for reconfigurable devices and components. MEMS switches are reliable in operation but not an economical solution as compared to the diodes. However, these face challenges of wear and tear of the mechanical part. Therefore, liquid crystal and graphene are exotic solutions for high frequencies, particularly for terahertz (THz) frequencies. There are many applications of liquid crystal- and graphene-based transmitarrays reported in the literature [41][42][43]. They are feasible for phase integration, their small size and low biasing complexity at lower to higher frequencies. Due to their advantage of

being able to vary the transmission phase change freely, most of the beam forming/beam steering reconfigurable transmitarrays are designed by the former method. However, there is a disadvantage of the overall radio performance of the transmitarray antenna that may deteriorate due to its complexity of implementation or the additional loss of active elements. The latter method structurally changes the wavefront shape of the source antenna electrically or mechanically and has the advantage of structurally fixing the TA. However, there is a disadvantage of a large motor for arrays as mentioned in [44][45][46][47][48].

Significant research has been conducted in recent years [49][50][51][52][53]. A transmitarray antenna has been implemented with a source antenna (horn, microstrip patch antenna) and a planar array. The working principle of a transmitarray antenna uses a high transmittance and a transmission phase change characteristic of more than 360 degrees to control the wavefront of the source antenna. This type of transmitarray antenna is a high gain antenna and is beam forming, beam steering, and multi-beam [54][55][56]. It is designed as a beam control system such as PIN diodes, varactors, MEMS systems, and microfluids. These reconfigurable devices can be used in many applications. In order to perform beam forming/beam steering in the desired direction, it can be roughly divided into two methods. The total wavefront of the transmitarray antenna can be calculated as the sum of the wavefront of the source antenna and the wavefront of the plane wave passing through the transmitarray. This point is used to implement beam steering by a transmitarray with variable transmission phase change or when the wavefront shape of the source antenna is applied.

2. Beam Steering/Beam Forming Principle of Transmitarray

The transmitarray antenna is an antenna that is capable of modifying the radiation pattern of a directional antenna such as a patch antenna or a horn antenna. A transmitarray has the capability of adjusting the wavefront of the source antenna and the incident wave. By using a structure that can adjust the size and phase of the incident wave, the transmission antenna can be used in various fields such as beam steering, beam focusing, and polarization control. **Figure 1** shows a typical radiation model of a transmission antenna composed of a source antenna and a transmitarray. A transmitarray is formed by a feed, which is labeled as a source antenna where the source antenna is placed at a distance F from transmitarray. Focal distance (F) is calculated as a tradeoff between spillover losses and an increase in gain, aperture efficiency, and other parameters. The source antenna illuminated by incident wave to the first part of the array is called the receiver. The receiver is directly connected to group of phase shifters to control the beam wave front in the required direction. The other end of the phase shifters are coupled with a transmitter layer, which produces a phase shift in the incident wave that works in transmitter mode. The phase shifter of each unit cell provides γn path difference to the source point to obtain the desired scan angle θ. As shown in **Figure 1**, the direction of the incident wave is determined by radiation controlled by the transmission phase of the transmitarray. Transmitarrays are generally composed of several resonant unit cells with a spatial periodicity that forms a planar arrangement.

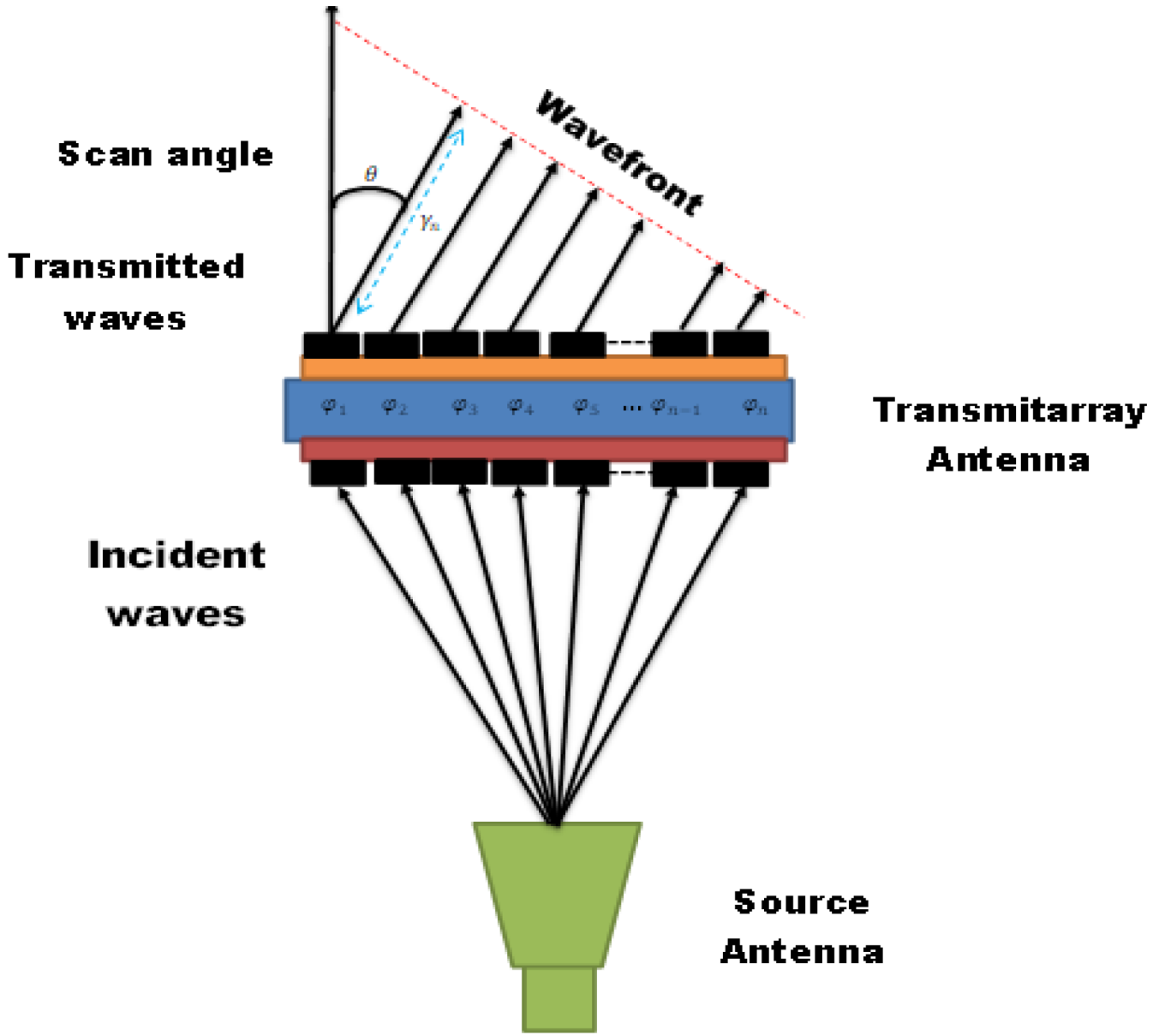

Figure 1. Generic radiation model of transmitarray antenna.

The principle of beam forming/beam steering transmitarrays is reported in [57][58][59][60][61][62]. There are incident EM waves generated from a feed source that passes through a transmitarray made up of nth (n = 0, 1, …) elements of periodicity of "a" and produces phase change φ_n shown in Equation (1).

$$\varphi_n = k_o n\, \Delta s + \varphi_0 \quad (1)$$

where $k_\circ = 2\pi/\lambda_0$ is the propagation constant of the free space-waves. Δs is the path difference between the nth and (n + 1th) elements after they pass through the transmitarray. Δs is defined here for the deflection angle θ of the

transmitted wave with element dimensions a that is the path difference with the deflection angle Δs = a.sinθ. Now researchers can write the phase change as $\varphi_n = \varphi_{n+1} - \varphi_n$.

$$\Delta\varphi = k_{\circ}\Delta s = \frac{2\pi}{\lambda_0}.\,a.\,\sin\theta \quad (1)$$

(2)

$$\sin\theta = \frac{\lambda_0}{2\pi a}.\ \Delta\varphi \quad (2)$$

(3)

Equations (2) and (3) demonstrate that if researchers define the deflection angle θ, researchers can calculate the phase change Δφ from Equation (2). Thus, both equations show inter-dependent relations for each other [63]. Similarly, the design and implementation of beam switching in arrays using a butler matrix have also been reported [64][65][66].

Transmitarray unit cells are usually designed based on microstrip patches, meta-materials [67][68], and frequency selective surfaces (FSS) [69][70]. The microstrip patch metasurface of the unit cell and its permeation characteristics are shown in [71]. The unit cell comprises of four dielectrics and five circular metal patches, and the equivalent circuit model can be expressed by series inductance and parallel capacitance in the passband. The transmission characteristics of the metasurface can be controlled by the radius (a) of the metal circular patch and the transmittance and transmission phase of the circular microstrip patch array transmitarray at 5.8 GHz. In this case, the size (W) of the square unit cell is 20 mm (0.38 λ_0), the dielectric constant (εr) and thickness (h) of the dielectric substrate are 2.2 and 3.2 mm, respectively. From 1 mm to 9.1 mm, a transmittance of 0.8 or more and a change in transmission phase of about 400 degrees can be obtained. A high gain transmission antenna using a metasurface composed of 10 × 10 circular patch array unit cells is presented. The total size of the transmitarray is 200 mm (about 4 λ_0), and the distance between the source antenna and the metasurface is 50 mm (about 1 λ_0).

The total wavefront of the transmitarray antenna can be conceptually expressed as the sum of the wavefront of the source antenna and the transmission phase of the transmitarray, as illustrated in **Figure 2**. When the focal source antenna and transmitarray antenna are fixed for phase implementing high gain and shape of the wavefront, a straight line is demonstrated in **Figure 2**a. The focal source antenna is fixed, whereas phase change is implemented by an active transmitarray in **Figure 2**b. A high gain variable phase change is achieved in this scenario by changing the wavefront of the active transmitarray. It is illustrated in **Figure 3** that the wavefront of the transmitarray antenna is fixed through the change in the wavefront shape of the source antenna using the phase

transformation surface that helps to implement the change of phase and achieve the high gain steering transmitarray. Aperture efficiency is an important performance indicator of a transmitarray antenna. Aperture efficiency (η_a) is defined in terms of the taper efficiency (η_t), spillover efficiency (η_s), polarization efficiency (η_{pol}), transmission efficiency (η_{tran}), phase efficiency (η_{ph}), and random surface as in Equation (4). It can be calculated as the product of the error efficiency (η_r) [72].

$$\eta_a = \eta_t . \eta_s . \eta_{pol} . \eta_{tran} . \eta_{ph} . \eta_r \quad (3)$$

(4)

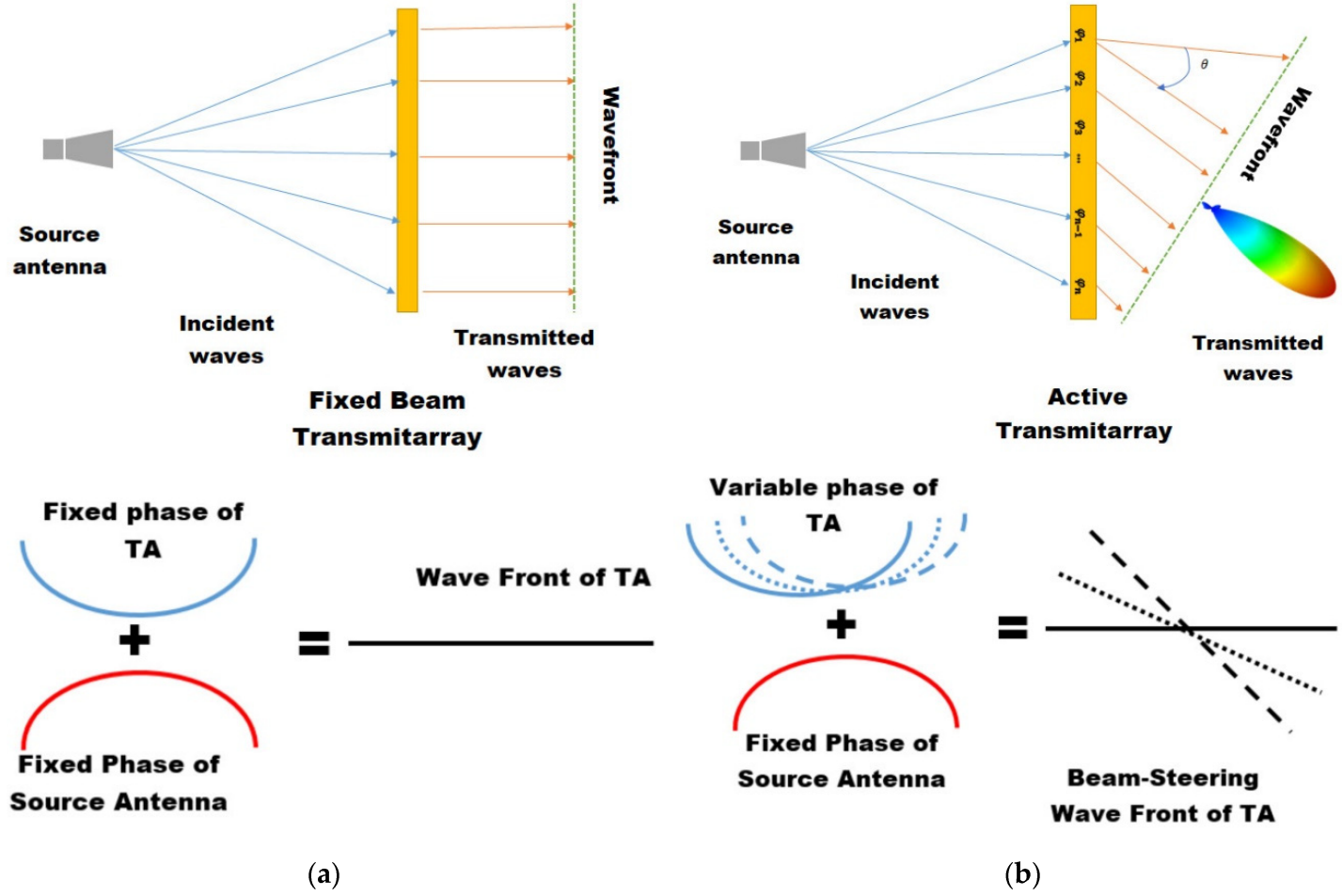

Figure 2. Conceptual diagram of the wavefront of (**a**) fixed beam transmitarray and fixed source antenna (**b**) active transmitarray with fix source and variable phase shift of TA.

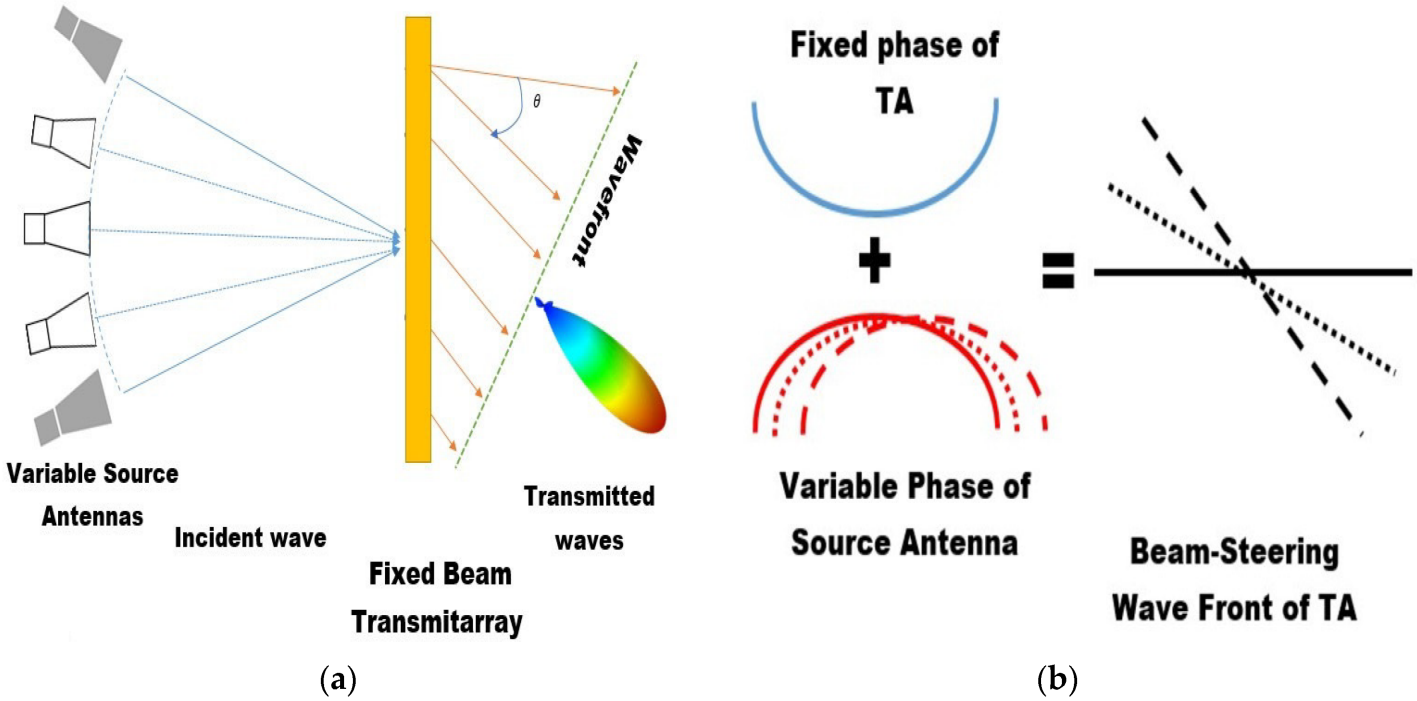

Figure 3. (**a**) Conceptual diagram of the wavefront of fixed beam transmitarray and variable source antenna; (**b**) phase variation concept of fixed transmitarray and variable source antenna.

Here, the efficiencies that mainly affect the aperture efficiency of the transmitarray antenna are the taper efficiency and the spillover efficiency. These two efficiencies are determined by the size and spacing of the source antenna and the metasurface. Taper and spillover efficiencies are related to the uniformity and amount of power reaching the metasurface from the source antenna, respectively, and are calculated by Equations (5) and (6).

$$\eta_t = \frac{\eta_a}{S} \frac{\left| \int E(x,y)^2 . dS \right|^2}{\int \left| E(x,y)^2 dS \right|} \quad (4)$$

(5)

$$\eta_s = \frac{\int \left| E(x,y)^2 dS \right|}{P_{rad}} \quad (5)$$

(6)

where S and P_{rad} are the area of the metasurface and the radiation power of the source antenna, respectively. It is vital to determine the source antenna, the distance between the source antennas and the plane array (F), and the

size (D) of the transmitarray to optimize the aperture efficiency of the transmitted antenna using the TA.

When the distance between the source antenna and the plane array is short, the spillover efficiency is high but the taper efficiency is low. Conversely, if F becomes longer, taper efficiency is high but spillover efficiency is lower. In addition, as the size of the transmitarray increases, the spillover efficiency is high but the taper efficiency decreases. Therefore, to maximize the aperture efficiency of the transmit antenna, it is necessary to optimize F/D. Maximum numerical aperture efficiency and the optimum gain of the source antenna following various F/D are shown in [42]. In this case the gain of the source antenna has become relatively low, the maximum value of the aperture efficiency decreases, but the distance F with maximum efficiency is reduced and a low-profile transmitarray antenna can be designed. In addition, a source antenna with a high gain may be applied to secure the maximum aperture efficiency, for example, when a patch antenna having a gain of 7.5 dBi is applied to a transmission antenna as a source antenna, the maximum aperture efficiency is about 62%, and F/D can be designed to 0.2.

3. Beam Steering/Beam Forming Using Reconfigurable Components

Several studies are available in the literature [73][74][75][76][77][78][79][80] to demonstrate the operations and functions of transmitarray beam steering. These are realised by utilizing different reconfigurable devices, materials, element designs, and operational parameters. However, every structure needs a requisite to obtain the beam steering/beam forming of the transmitarray antenna. Each transmitarray unit cell must acquire a transmission phase that can be tuned (varied) up to 360 degrees. Moreover, the transmission coefficient should remain constant throughout the operational bandwidth. This section focuses on demonstrating the electronically reconfigurable beam of transmitarray, transmission phase distribution on the transmitarray surface, and the phase shift of each unit cell. Reconfigurable beam steering can be achieved with different techniques. The most prominent one is electronic control accomplished, which is achieved by loading one or more active devices into the resonant elements designed on the unit cell such as (PIN diodes, varactors, and MEMS switches). Other techniques are on the utilization of tunable materials (liquid crystal, microfluidic systems). There is a detail Summary of beam steering reconfigurable transmitarrays with PIN diodes is presents in **Table 1**.

Table 1. Summary of beam steering reconfigurable transmitarrays with PIN diodes.

Ref.	Unit Cell Technique	Phase Control Device	Frequency (GHz)	Polarization	Phase Range	Gain (dBi)	Aperture Efficiency (%)	Band Width	Beam Scanning Capacity
[32]	PCB stacked patch	PIN diode	5.4	LP, CP	1-B1T	17	28.5	8.5	±50° E and H plane
[73]	O-U slot patches	PIN diode	29	CP	1-B1T	28.5	9.5	14.6%	±60° E and H

Ref.	Unit Cell Technique	Phase Control Device	Frequency (GHz)	Polarization	Phase Range	Gain (dBi)	Aperture Efficiency (%)	Band Width	Beam Scanning Capacity
									plane
[74]	double O-slot patches	PIN diode	29	LP	2-B1T	19.8	15.9	16.2%	±60° E and H plane
[76]	microstrip Vivaldi	PIN diode	13.6	LP	1-B1T	22.3	25.6	1.9% (1-dB)	±40° E and H plane
[79]	coupled slot	PIN diode	12.5	LP	1-B1T	17	14	9.6%	±50° E and H plane
[80]	Square ring patch	PIN diode	5.75	CP	1-BIT	14	–	2.5%	±30° E and H plane
[81]	H and I shape coupling slot	PIN diode	12.5	LP	1-BIT	17	14	9.6%	±50° E and H plane
[82]	C-shaped probe-fed patch	PIN diode	12.1	LP	1-B1T	22.1	22.2	16%	±60° E and H plane
[83]	split circular rings	PIN diode	5	LP	1-B1T	16.8	18.4	17% (1-dB)	±40° E and H plane
[84]	multilayer annular [73] ring patches	PIN diode	14	LP	1-B1T	20.4	33.4	33%	±50° E and H plane

it cell. A
nape slot,
and two PIN diodes are mounted to the microstrip patch element. The receiver patch has etched on another O slot patch connected to a transmitter patch with a metallic via that transfer electromagnetic energy to the transmitter. This unit cell achieves 10.1–12.1% 3 dB transmission bandwidth. This entry is further extended in [74][75] to validate the array parameters of this technique. There are two transmitarrays of 14 × 14 and 20 × 20, reported as switchable circular and linear polarization. These are 1-bit and 2-bit phase resolution variable (tunable) unit cells. There are two and four PIN diodes mounted that allow transmission phase control for each design, respectively. The 1-bit prototype reconfigurable unit cell's measured gain is 20.8 dBi with a 3 dB transmission bandwidth of 14.6% at 29 GHz. The 2-bit design has a measured gain of 19.8 dBi with a 3 dB bandwidth of 16.2% at 29 GHz.

Moreover, a novel reconfigurable Yagi–Vivaldi transmitarray structure was reported in [76][77] for beam steering of the transmitarray at Ku-band. This reconfigurable transmitarray (RTA) primarily focused on a wide bandwidth and beam scanning at Ku-band. The RTA unit cell contains a tightly coupled microstrip. A Vivaldi antenna based on the transmitter and a Yagi antenna structure etched on it behaves as a transmitter. A pair of anti-parallel diodes are

mounted on a slot-line to the microstrip phase shifter to obtain 180° phase shift with the current reversal mechanism shown in **Figure 4**. It achieves 14% 1 dB bandwidth of a reconfigurable transmitarray with peak gain 22.3 dBi at 13.6 GHz. The RTA realized 25.6% aperture efficiency with ±60 degrees scan angle for both E-plane and H-plane. Two novel linearly polarized reconfigurable design transmitarrays have been investigated with PIN diode at Ku-band in [78][79]. An asymmetric dipole element PIN diode-based reconfigurable transmitarray is presented in [79]. This novel design has been investigated as a 1-bit dual-band linearly polarized reconfigurable transmitarray at Ku-band, as shown in **Figure 5**. This element has an active dipole for the receiver and an asymmetric passive dipole for the transmitter 1-bit transmission phase shift, obtained by integrating two diodes on an active patch in the reverse direction with the current reversal mechanism. To reduce the impact of diode resistance and improve insertion loss, two parasitic bypass dipoles alongside the main patches can be added. The dual-polarization parameter is realized by orthogonal interconnecting for the transmitter and receiver. A 10 × 10 elements array is designed, manufactured, and tested. It achieves measured aperture efficiency of 22.6% with a peak gain of 18.3 dB at 12.2 GHz. The 2D beam steering feature correspondence realized in a test environment with a scanning angle covers ±50 degrees. The maximum measured E-Plane and H-plane losses are 2.9 dB and 3.5 dB, respectively, as shown in **Figure 5**c.

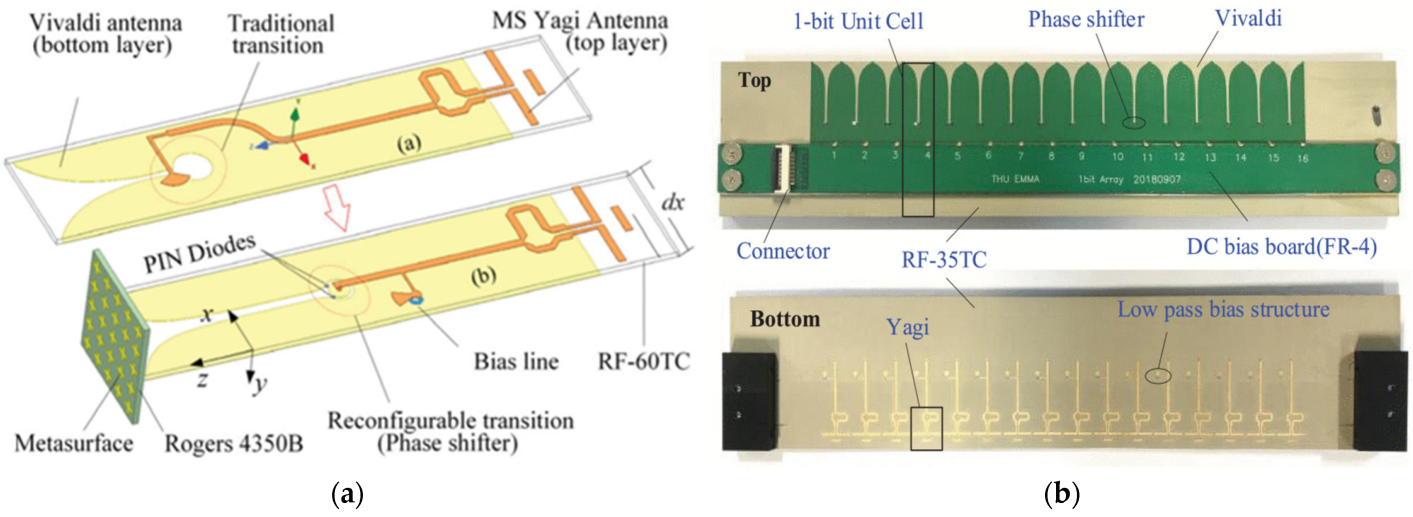

Figure 4. (**a**) Geometry of Vivaldi reconfigurable transmitarray with WIAM metasurface; (**b**) fabricated 1 × 16 subarray prototype (reprinted with permission of [76]. Copyright 2021 Xiao, Y., et al.).

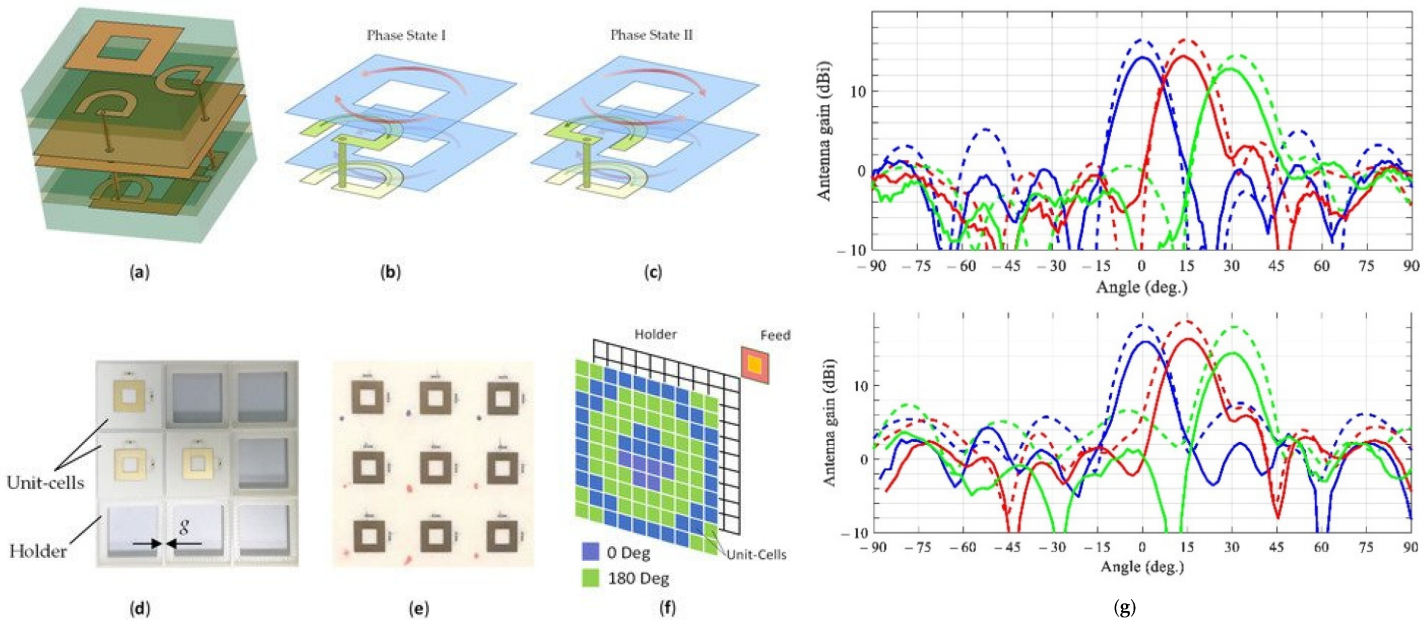

Figure 5. Geometry of 3 × 3 1 bit RTA element with biasing circuit; (**a**–**f**) exploded view, top view; (**g**) measures radiation pattern of E-plane and H-plane, respectively (reprinted with permission of [80]. Copyright 2021 Kozlov, D., et al.).

Another novel C-band design of a transmitarray is discussed in [80], and some other applications of this array are explored in [80][85][86]. A C-band square ring patch with proximity coupled U-shape resonator transmitarray is proposed. A prototype of a 1-bit beam steering 10 × 10 transmitarray with performance is presented. A prototype of a square ring patch with a proximity coupled U-shape resonator with good/bad effects is also demonstrated. The dual-polarized beam scanning effect is experimentally verified in the test setup. The maximum measured gain of the proposed transmitarray is 12 dBi, corresponding to maximum scan loss that reaches 2 dB with a scan angle of ±30 degrees.

Furthermore, a novel architecture of a reconfigurable coupling slot transmitarray is mentioned in [81]: a prototype of a 1-bit electronically reconfigurable transmitarray for Ku-band. Two orthogonal H-shape slots were integrated on patches that act as transmitter and receiver, respectively. Electromagnetic energy was transmitted by coupling a transmit line in between slot patches. Diodes were mounted on the coupling line to realize the electronic phase control in an anti-parallel direction to produce 180° phase difference. The oblique incidence performance of the elements was maintained by sub-wavelength element spacing $\lambda_0/3$. A 16 × 16 element 12.5 GHz reconfigurable transmitarray was designed and tested. The maximum gain of 17.0 dBi corresponds to an aperture efficiency of 14.0% presented in experimental results. The H-shape coupling slot transmitarray realizes a beam scanning angle within ±50 degrees for E- and H-planes. The 3 dB gain bandwidth retains 9.6% in the measured results.

This work is further improved in [82]: a 16 × 16 elements reconfigurable transmitarray is proposed in this entry. The transmitter is designed as a C-shape feed probe placed beneath a rectangular patch to obtain the feathers of broad bandwidth and lower insertion loss. The receiver of the transmitarray is a U-shaped slot etched on a simple rectangular patch. To induce a reverse current path, two PIN diodes are symmetrically placed on the feed probe of

the unit cell shown in **Figure 6**. The minimum measured insertion loss is realized at 0.47 dB for each phase state with 16% of 3 dB broad bandwidth achieved by stepped impedance matching performance. There are 256 elements in the feed shape probe transmitarray with 512 PIN diodes used in its manufacturing and testing. The maximum peak gain is 22.1 dBi at 12.5 GHz with an aperture efficiency of 21.2%. The 3 dB insertion bandwidth is realized at 12.3% with electronic beam scanning performance of ±60 degrees for two-dimensional H- and E-planes, respectively. This novel reconfigurable transmitarray is a good solution for many applications in wireless communication systems.

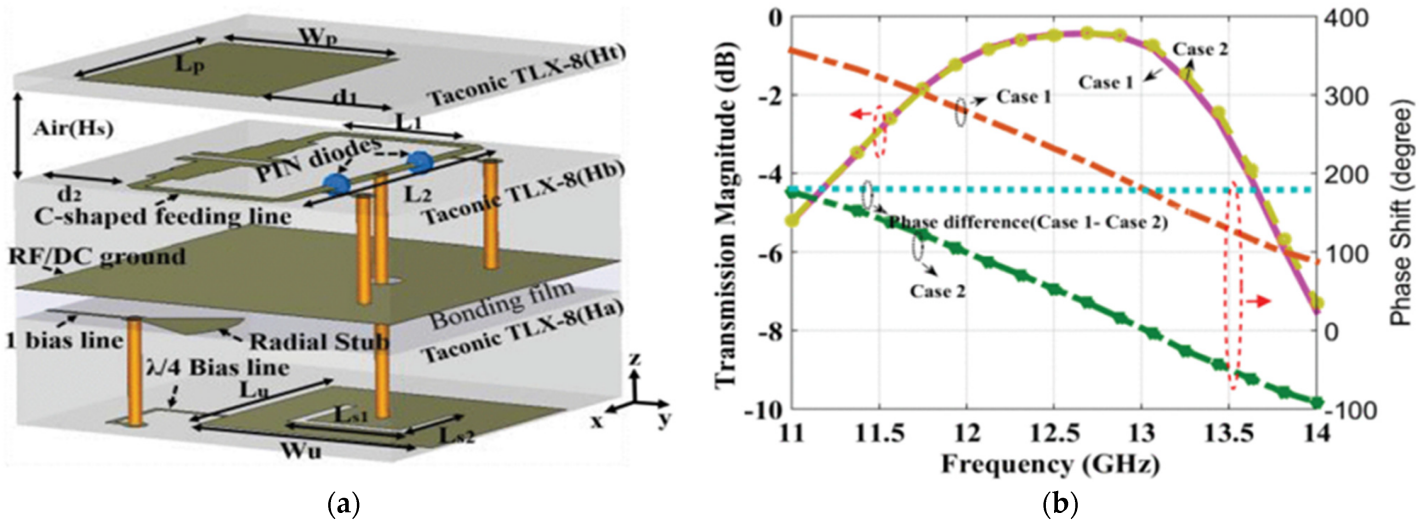

Figure 6. (**a**) Exploded view of the proposed unit cell; (**b**) simulated results of transmission magnitude and phase shift (reprinted with permission of [82]. Copyright 2020 Wang, M., et al.).

Another advanced technique structure of a transmitarray is reported in [83] with a polarization rotation unit cell. Two split circles are connected with two narrow strips with pin diodes mounted in between them. Polarization control structures sandwich the PIN diode loaded with a transmitter and receiver. The air gap is presented between the transmitter and receiver to mount diodes on patches easily, and bias circuits are etched on the polarization control structure. The phase difference 180° is achieved for two outgoing polarized waves for 0 and 180 degree phase states. The polarization control structure reduces the blocking effect of dc-bias lines and improves the aperture efficiency of the structure. A 16 × 16 1-bit transmitarray is designed, fabricated, and tested in a test setup. Two-dimensional electronic beams scanning of ±40 degrees is realized by the polarization rotation element. The maximum measure 3 dB and 1 dB insertion loss of 45% and 17% are obtained, respectively, at 5.5 GHz. The aperture efficiency of the polarization rotation transmitarray is 18.4%.

In [84], the authors have presented a 10 × 10 elements 1-bit reconfigurable transmitarray (RTA) with linear polarization at Ku-band. This transmitarray has the ability of beam steering for a wide range of frequencies. The reported unit cell consists of multiple-layer circular rings and substrates. Every element of the RTA has the capability to electronically control phase shift path difference for 0 and 180 states. The 3 dB gain bandwidth of the structure lies at 33% (12.5 GHz–17.5 GHz) at 15 GHz frequency. The effective aperture efficiency of the annular

rings RTA is achieved up to 33.64% at 15 GHz. From 14 GHz to 17 GHz, two-dimensional beam steering with ±60 degrees may be realized.

3.2. Varactor Diodes

The entry also presents the reconfigurable transmitarray (RTA) made up of varactors to accomplish beam forming/beam steering [87][88][89][90][91][92]. Varactor diodes are the best solution for continuous tuning by using electronic switches. Varactor diodes are mature technology; they are economical, have low insertion losses, can be modeled easily, and have voltage control switches. There are a wide range of diodes that can be used related to applications shown in **Figure 7**. It is important to choose the varactor diode that offers the best performance for many applications. A varactor diode capacitance ratio is defined as C_{max}/C_{in}, meaning a large capacitance ratio results in a wide range of tuning capacitance. There is a detail Summary of beam steering reconfigurable transmitarrays with varactor diodes shown in **Table 2**.

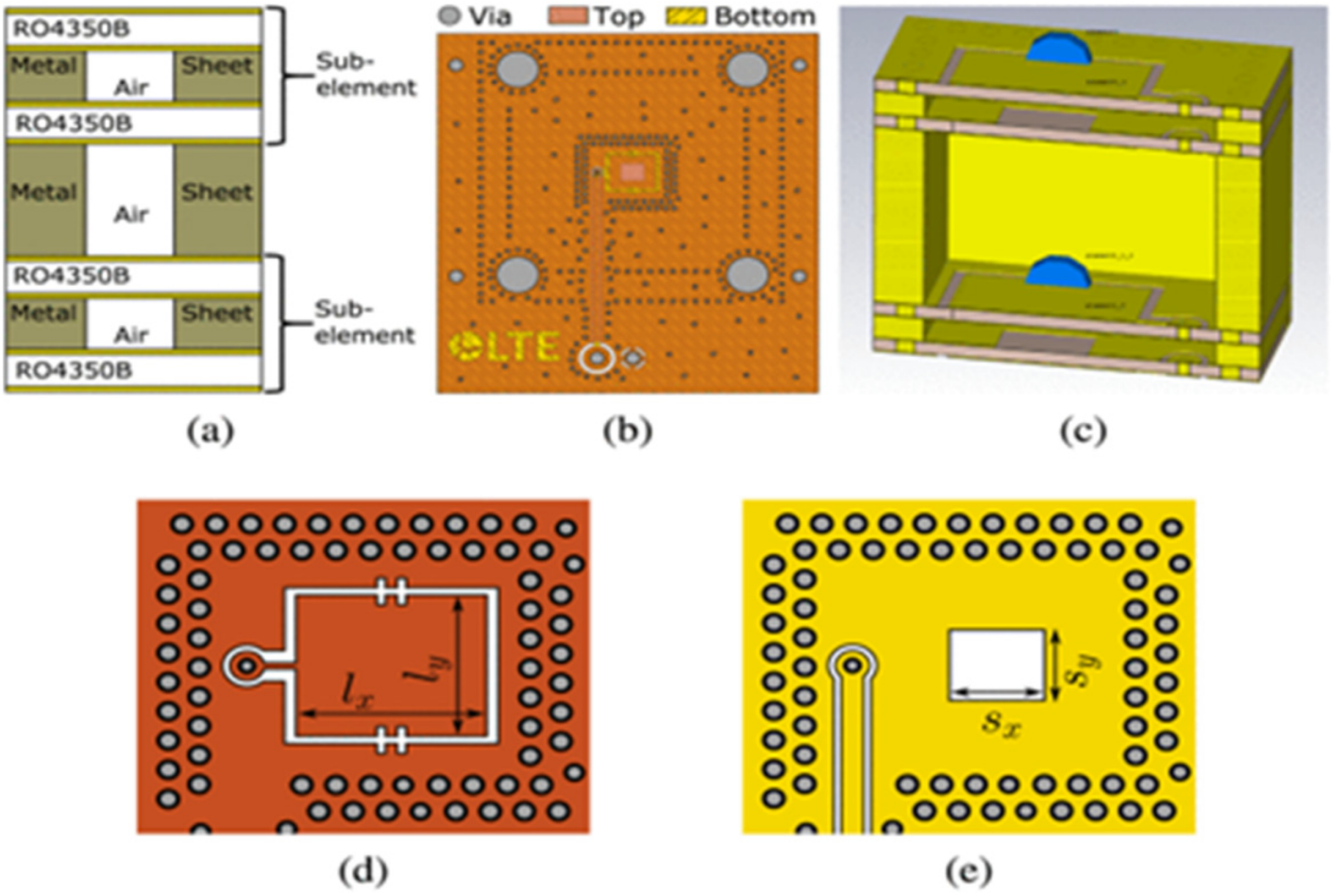

Figure 7. (**a**) Layer stack view of proposed unit cell, (**b**) layout view, (**c**) 3D view, (**d**) top layer, (**e**) bottom layer (reprinted with permission of [93]. Copyright 2019 Frank, M., et al.).

Table 2. Summary of beam steering reconfigurable transmitarrays with varactor diodes.

Ref	Unit Cell Technique	Phase Control Device	Frequency (GHz)	Polarization	Phase Range	Gain (dBi)	Aperture Efficiency	Band Width	Beam Steering Capacity
[93]	stacked layers	varactor diode	24.6	LP	360°	_	_	1 GHz	±50° E and H plane
[94]	compact varactor based phase shifters	varactor diode	5.6	LP	360°, 1-BIT	15.7	33.3	16.7%	60° E and H plane
[95]	FSS	varactor diode	5.2	LP	480°	20.2	_	13%	±30° E and H plane
[96]	integrated leaky wave	varactor diode	4.8	LP	400°	15.6	34	9% [97][93]	±45° E and H plane

steering performance. Each element of the transmitarray is composed of four substrate Rogger RO4350B double sided layers, shown in **Figure 7**. One pair can be tuned for 180° phase shift control, and a whole pair of unit cells duplicated to earn 360° phase shift. The electronic phase control of the element is obtained by loading each layer with varactor diodes. A theoretical 3 dB bandwidth of the unit cell is 1 GHz at 24.6, as mentioned in this entry, but it reveals that the insertion loss of this entry achieves −5 dB. Experimental results show that 3 dB insertion losses are quite high up to −12 dB for this transmitarray. Furthermore, this work is extended in [93] and an array of 6 × 6 elements of the abovementioned transmitarray is fabricated. This RTA has the experimental performance of beam scanning capability ±50 degrees at 24.6 GHz in both the H-plane and E-plane.

Another novel varactor diode and pin diode base phase shifter transmitarray design is reported in [94]. A wideband varactor diode and pin diode base phase shifter reconfigurable transmitter gives continuous phase shift control at 5.8 GHz. This multilayer element structure transmitter (Tx) comprises an H-slot rectangular patch integrated with two diodes. A varactor diode is mounted on the receiver layer to build a 180° analog phase shifter combined with pin diodes to acquire 360° electronic phase shift. Theoretical transmission insertion loss includes 0.85 dB to 1.24 dB at 5.8 GHz frequency. A 3 dB bandwidth is obtained up to 17% of the required frequency. A 16 × 16 elements prototype of the transmitarray is designed, fabricated, and measured result tested. A maximum peak gain of 23.7 dBi at 5.8 GHz is achieved using the varactor diode-based phase shifter transmitarray. The 2D transmitarray beam scanning performances are maintained for ±60 degrees elevation and azimuth planes.

In addition, a frequency selective surface (FSS) varactor diode reconfigurable transmitarray with 2D beam scanning ability is reported in [95]. Each layer of the FSS loaded with a varactor diode enables beam scanning of the main beam of the original radiation pattern in both the E-plane and H-plane. A five-layer 5 × 5 FSS transmitarray integrated with varactor diodes coupled with a horn antenna feed network has been verified with theoretical and experimental results. Two simulated and fabricated models are developed with a peak gain of 20.2

dBi and 19.9 dBi, respectively, at 5.8 GHz frequency. Experimental results of 2D beam steering are realized approximately ±30 degrees in both the azimuth and elevation planes. The proposed RTA shows the potential for use in applications with better economical fabrication cost compared to the most direct alternative beam steering approaches.

A detailed case study has been presented in [98] of the practical constraints of two-dimensional beam steering using a varactor diode-based meta-material at micro and mm-wave frequencies. The practical impacts of the varactor diode utilized with a meta-material-based RTA are deeply observed, as shown in **Figure 8**.

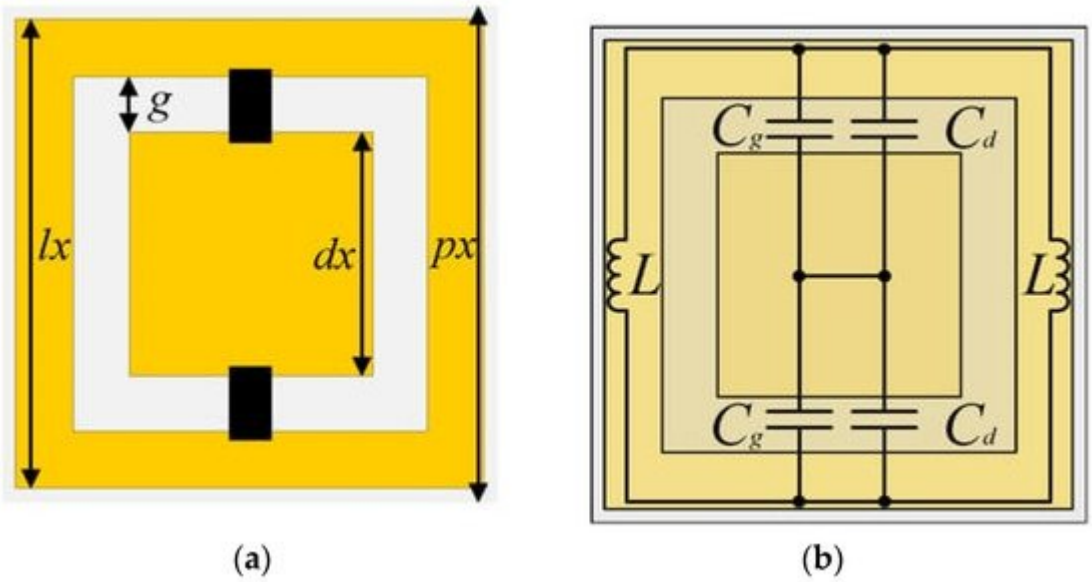

Figure 8. (**a**) FSS proposed unit cell; (**b**) equivalent circuit diagram (reprinted with permission of [98]. Copyright 2021 Reis, J.R., et al.).

Four prototypes are developed on different frequencies, including 5, 14, 28, and 60 GHz, to understand the effect of internal resistance Rs and internal inductance Ls of varactor diodes. It is concluded from the above study that internal resistance Rs have various impacts on RTAs. On the other hand, internal inductance Ls affects the proposed TA's bandwidth and operational frequency band response. As internal inductance Ls increases, higher frequencies shift towards lower frequencies, increasing the bandwidth of the reported elements. These result in a reduction in the overall phase shift accomplished by multilayers of unit cells that may have the impact of reducing the scanning range of TAs to perform beam steering with a transmitarray.

References

1. Alibakhshikenari, M.; Virdee, B.S.; See, C.H.; Abd-Alhameed, R.A.; Falcone, F.; Limiti, E. High-Isolation Leaky-Wave Array Antenna Based on CRLH-Metamaterial Implemented on SIW with ±30° Frequency Beam-Scanning Capability at Millimetre-Waves. Electronics 2019, 8, 642.

2. Alibakhshikenari, M.; Virdee, B.S.; Khalily, M.; Shukla, P.; See, C.H.; Abd-Alhameed, R.; Falcone, F.; Limiti, E. Beam-scanning leaky-wave antenna based on CRLH-metamaterial for millimetre-wave applications. IET Microw. Antennas Propag. 2019, 13, 1129–1133.
3. Alibakhshi-Kenari, M.; Andújar, A.; Anguera, J. New compact printed leaky-wave antenna with beam steering. Microw. Opt. Technol. Lett. 2016, 58, 215–217.
4. Bia, P.; Caratelli, D.; Mescia, L.; Gielis, J. Analysis and synthesis of supershaped dielectric lens antennas. IET Microw. Antennas Propag. 2015, 9, 1497–1504.
5. Hwang, S.; Lee, B.; Kim, D.H.; Park, J.Y. Design of S-band phased array antenna with high isolation using broadside coupled split ring resonator. J. Electromagn. Eng. Sci. 2018, 18, 108–116.
6. Rudge, A.; Adatia, N. New class of primary-feed antennas for use with offset parabolic-reflector antennas. Electron. Lett. 1975, 11, 597–599.
7. Kock, W. Path-length microwave lenses. Proc. IRE 1949, 37, 852–855.
8. McGrath, D. Planar three-dimensional constrained lenses. IEEE Trans. Antennas Propag. 1986, 34, 46–50.
9. Pozar, D. Flat lens antenna concept using aperture coupled microstrip patches. Electron. Lett. 1996, 32, 2109–2111.
10. Liu, X.; Peng, L.; Liu, Y.F.; Yu, W.S.; Zhao, Q.X.; Jiang, X.; Li, S.M.; Ruan, C. Ultrabroadband All-Dielectric Transmitarray Designing Based on Genetic Algorithm Optimization and 3-D Print Technology. IEEE Trans. Antennas Propag. 2020, 69, 2003–2012.
11. Afzal, M.U.; Esselle, K.P.; Lalbakhsh, A. A Methodology to Design a Low-Profile Composite-Dielectric Phase-Correcting Structure. IEEE Antennas Wirel. Propag. Lett. 2018, 17, 1223–1227.
12. Yu, W.-S.; Peng, L.; Liu, Y.-F.; Zhao, Q.-X.; Jiang, X.; Li, S.M. An Ultra-wideband and High Aperture Efficiency All-Dielectric Lens Antenna. IEEE Antennas Wirel. Propag. Lett. 2021, 20, 2442–2446.
13. Godi, G.; Sauleau, R.; Le Coq, L.; Thouroude, D. Design and Optimization of Three-Dimensional Integrated Lens Antennas with Genetic Algorithm. IEEE Trans. Antennas Propag. 2007, 55, 770–775.
14. Fan, Y.; Xu, Y.; Qiu, M.; Jin, W.; Zhang, L.; Lam, E.; Tsai, D.; Lei, D. Phase-controlled metasurface design via optimized genetic algorithm. Nanophotonics 2020, 9, 3931–3939.
15. Zhao, X.; Yuan, C.; Liu, L.; Peng, S.; Qiang, Z.; Zhou, H. All-Metal Transmit-array for Circular Polarization Design Using Rotated Cross-Slot Elements for High Power Microwave Applications. IEEE Trans. Antennas Propag. 2017, 65, 3253–3256.

16. Chen, G.T.; Jiao, Y.C.; Zhao, G. Novel wideband metal-only transmitarray antenna based on 1-bit polarization rotation element. Int. J. RF Microw. Comput.-Aided Eng. 2020, 30, e22388.
17. Abdelrahman, A.H.; Elsherbeni, A.Z.; Yang, F. Transmitarray antenna design using cross-slot elements with no dielectric substrate. IEEE Antennas Wirel. Propag. Lett. 2014, 13, 177–180.
18. Zhao, J.; Li, T.; Li, H.; Yang, X.; Zhou, Y.; Mao, W.; Wang, H.; Hu, B.; Zou, H.; Liu, Q. A Novel Planar Mode-Transducing Antenna Based on Metal-Only Transmitarray Surfaces. IEEE Trans. Antennas Propag. 2019, 67, 3762–3773.
19. Liu, G.; Wang, H.J.; Jiang, J.S.; Xue, F.; Yi, M.A. high-efficiency transmitarray antenna using double split ring slot elements. IEEE Antennas Wirel. Propag. Lett. 2015, 14, 1415–1418.
20. Guerra, A.; Guidi, F.; Clemente, A.; D'Errico, R.; Dussopt, L.; Dardari, D. Application of transmitarray antennas for indoor mapping at millimeter-waves. In Proceedings of the 2015 European Conference on Networks and Communications (EuCNC), Paris, France, 29 June–2 July 2015; IEEE: Piscataway, NJ, USA, 2015.
21. Santini, T.; Zhao, Y.; Wood, S.; Krishnamurthy, N.; Kim, J.; Farhat, N.; Alkhateeb, S.; Martins, T.; Koo, M.; Zhao, T.; et al. In-vivo and numerical analysis of the eigenmodes produced by a multi-level Tic-Tac-Toe head transmit array for 7 Tesla MRI. PLoS ONE 2018, 13, e0206127.
22. Rappaport, T.S.; Sun, S.; Mayzus, R.; Zhao, H.; Azar, Y.; Wang, K.; Wong, G.; Schulz, J.K.; Samimi, M.; Gutierrez, F. Millimeter Wave Mobile Communications for 5G Cellular: It Will Work! IEEE Access 2013, 1, 335–349.
23. Jouanlanne, C.; Clemente, A.; Huchard, M.; Keignart, J.; Barbier, C.; Le Nadan, T.; Petit, L. Wideband Linearly Polarized Transmitarray Antenna for 60 GHz Backhauling. IEEE Trans. Antennas Propag. 2017, 65, 1440–1445.
24. Zainud-Deen, S.H.; Hassan, W.; Malhat, H. Near-Field focused folded transmitarray antenna for medical applications. Wirel. Pers. Commun. 2017, 96, 4885–4894.
25. Hassanien, A.; Vorobyov, S.A.; Yoon, Y.S.; Park, J.Y. Root-MUSIC based source localization using transmit array interpolation in MIMO radar with arbitrary planar arrays. In Proceedings of the 2013 5th IEEE International Workshop on Computational Advances in Multi-Sensor Adaptive Processing (CAMSAP), Saint Martin, France, 15–18 December 2013; IEEE: Piscataway, NJ, USA, 2013.
26. Veljovic, M.J.; Skrivervik, A.K. Circularly Polarized Transmitarray Antenna for CubeSat Intersatellite Links in K-Band. IEEE Antennas Wirel. Propag. Lett. 2020, 19, 1749–1753.
27. Chen, Q.; Saifullah, Y.; Yang, G.-M.; Jin, Y.-Q. Electronically reconfigurable unit cell for transmit-reflect-arrays in the X-band. Opt. Express 2021, 29, 1470–1480.

28. Li, W.; Wang, Y.; Sun, S.; Shi, X. An FSS-Backed Reflection/Transmission Reconfigurable Array Antenna. IEEE Access 2020, 8, 23904–23911.
29. Reis, J.; Al-Daher, R.Z.; Copner, N.; Caldeirinha, R.; Fernandes, T. Two-dimensional antenna beamsteering using metamaterial transmitarray. In Proceedings of the 2015 9th European Conference on Antennas and Propagation (EuCAP), Lisbon, Portugal, 12–17 April 2015; IEEE: Piscataway, NJ, USA, 2015.
30. Ali, Q.; Xiao, Y.; Sun, H. 1 BIT Wide-Band Hexagonal Electronically Reconfigurable Unit Cell for Ka-Band Transmit-array. In Proceedings of the 2020 IEEE Asia-Pacific Microwave Conference (APMC), Hong Kong, China, 8–11 December 2020; IEEE: Piscataway, NJ, USA, 2020.
31. Tang, J.; Xu, S.; Yang, F.; Li, M. Design of a Wideband Reconfigurable Transmitarrray Element Using a Novel Phase Shifter with Varactors and PIN Diodes. In Proceedings of the 2019 International Symposium on Antennas and Propagation (ISAP), Xi'an, China, 27–30 October 2019; IEEE: Piscataway, NJ, USA, 2019.
32. Ali, Q.; Xiao, Y.; Bin, X.; Sun, H.J. 1 BIT Fractal Hexagonal Shape Electronically Reconfigurable Transmit-array Unit Cell for 5G Communication Systems. In Proceedings of the 2021 1st International Conference on Microwave, Antennas & Circuits (ICMAC), Islamabad, Pakistan, 21–22 December 2021.
33. Huang, C.; Pan, W.; Ma, X.; Zhao, B.; Cui, J.; Luo, X. Using Reconfigurable Transmitarray to Achieve Beam-Steering and Polarization Manipulation Applications. IEEE Trans. Antennas Propag. 2015, 63, 4801–4810.
34. Clemente, A.; Dussopt, L.; Reig, B.; Sauleau, R.; Potier, P.; Pouliguen, P. 1-bit mems based reconfigurable unit-cell for transmit-array antennas at x-band frequencies. In Proceedings of the 13th International Symposium on RF MEMS and RF Microsystems (MEMSWAVE 2012), Antalya, Turkey, 2–4 July 2012.
35. Perez-Palomino, G.; Carrasco, E.; Cano-Garcia, M.; Hervas, R.; Quintana, X.; Geday, M.A. Design and Evaluation of Liquid Crystal-Based Pixels for Millimeter and Sub-Millimeter Electrically Addressable Spatial Wave Modulators. In Proceedings of the 2019 International Conference on Electromagnetics in Advanced Applications (ICEAA), Granada, Spain, 9–13 September 2019.
36. Li, X.; Li, Z.; Wan, C.; Song, S. Design and Analysis of Terahertz Transmitarray Using 1-bit Liquid Crystal Phase Shifter. In Proceedings of the 2020 9th Asia-Pacific Conference on Antennas and Propagation (APCAP), Xiamen, China, 4–7 August 2020; IEEE: Piscataway, NJ, USA, 2020.
37. Long, S.A.; Huff, G.H. A fluidic loading mechanism for phase reconfigurable reflectarray elements. IEEE Antennas Wirel. Propag. Lett. 2011, 10, 876–879.
38. Malhat, H.A.; Zainud-Deen, S.H.; Gaber, S.M. Circularly polarized graphene based transmitarray for terahertz applications. In Proceedings of the 2014 XXXIth URSI General Assembly and

Scientific Symposium (URSI GASS), Beijing, China, 16–23 August 2014; IEEE: Piscataway, NJ, USA, 2014.

39. Manzillo, F.F.; Smierzchalski, M.; Reverdy, J.; Clemente, A.A. Ka-band Beam-Steering Transmitarray Achieving Dual-Circular Polarization. In Proceedings of the 2021 15th European Conference on Antennas and Propagation (EuCAP), Online, 22–26 March 2021; IEEE: Piscataway, NJ, USA, 2021.
40. Clemente, A. Deliverable D3. 2: Electronically Reconfigurable Antenna; European Commission: Brussels, Belgium, 2017.
41. Minatti, G.; Martini, E.; Caminita, F.; Pavone, S.C.; Albani, M.; Toso, G.; Maci, S. Electronically reconfigurable metasurface antennas based on liquid crystal technology. In Proceedings of the 2019 13th European Conference on Antennas and Propagation (EuCAP), Krakow, Poland, 31 March–5 April 2019; IEEE: Piscataway, NJ, USA, 2019.
42. Hu, W.; Dickie, R.; Cahill, R.; Gamble, H.; Ismail, Y.; Fusco, V.; Linton, D.; Grant, N.; Rea, S. Liquid Crystal Tunable mm Wave Frequency Selective Surface. IEEE Microw. Wirel. Components Lett. 2007, 17, 667–669.
43. Hassan, W.M. Multilayer graphene-only transmitarray antenna (MGOT) for terahertz applications. In Proceedings of the 2017 34th National Radio Science Conference (NRSC), Alexandria, Egypt, 13–16 March 2017.
44. Lima, E.B.; Matos, S.A.; Costa, J.R.; Fernandes, C.A.; Fonseca, N.J.G. Circular Polarization Wide-Angle Beam Steering at Ka-Band by In-Plane Translation of a Plate Lens Antenna. IEEE Trans. Antennas Propag. 2015, 63, 5443–5455.
45. Rahmati, B.; Hassani, H.R. Low-Profile Slot Transmitarray Antenna. IEEE Trans. Antennas Propag. 2014, 63, 174–181.
46. Jiang, M.; Chen, Z.N.; Zhang, Y.; Hong, W.; Xuan, X. Metamaterial-Based Thin Planar Lens Antenna for Spatial Beamforming and Multibeam Massive MIMO. IEEE Trans. Antennas Propag. 2016, 65, 464–472.
47. Massaccesi, A.; Dassano, G.; Pirinoli, P. Beam scanning capabilities of a 3d-printed perforated dielectric transmitarray. Electronics 2019, 8, 379.
48. Lee, J.G.; Kwon, T.S.; Lee, J.H. Beam pattern reconfigurable circularly polarized transmitarray antenna by rearrangement of sources. Microw. Opt. Technol. Lett. 2019, 61, 999–1003.
49. Yeap, S.B.; Qing, X.; Chen, Z.N. 77-GHz dual-layer transmit-array for automotive radar applications. IEEE Trans. Antennas Propag. 2015, 63, 2833–2837.
50. Tuloti, S.H.R.; Rezaei, P.; Hamedani, F.T. High-efficient wideband transmitarray antenna. IEEE Antennas Wirel. Propag. Lett. 2018, 17, 817–820.

51. Bagheri, M.O.; Hassani, H.R.; Rahmati, B. Dual-band, dual-polarised metallic slot transmitarray antenna. IET Microw. Antennas Propag. 2017, 11, 402–409.
52. Chen, L.-W.; Ge, Y.; Bird, T.S. Ultrathin flat microwave transmitarray antenna for dual-polarised operations. Electron. Lett. 2016, 52, 1653–1654.
53. Tian, C.; Jiao, Y.-C.; Zhao, G. Circularly polarized transmitarray antenna using low-profile dual-linearly polarized elements. IEEE Antennas Wirel. Propag. Lett. 2016, 16, 465–468.
54. Xu, H.X.; Cai, T.; Zhuang, Y.Q.; Peng, Q.; Wang, G.M.; Liang, J.G. Dual-mode transmissive metasurface and its applications in multibeam transmitarray. IEEE Trans. Antennas Propag. 2017, 65, 1797–1806.
55. Abdelrahman, A.H.; Nayeri, P.; Elsherbeni, A.Z.; Yang, F. Single-Feed Quad-Beam Transmitarray Antenna Design. IEEE Trans. Antennas Propag. 2016, 64, 953–959.
56. Lee, C.; Hoang, T.V.; Chi, S.W.; Lee, S.; Lee, J. Low profile quad-beam circularly polarised antenna using transmissive metasurface. IET Microw. Antennas Propag. 2019, 13, 1690–1698.
57. Mailloux, R.J. Phased Array Antenna Handbook; Artech House: Norwood, MA, USA, 2017.
58. Reis, J.; Al-Daher, Z.; Copner, N.; Hammoudeh, A.; Caldeirinha, R.; Fernandes, T. Two-dimensional transmitarray beamsteering using stacked tunable metamaterials. In Proceedings of the 2014 Loughborough Antennas and Propagation Conference (LAPC), Loughborough, UK, 10–11 November 2014; IEEE: Piscataway, NJ, USA, 2014.
59. Abdelrahman, A.H.; Nayeri, P.; Elsherbeni, A.Z.; Yang, F. Analysis and Design of Transmitarray Antennas. Synthesis Lectures on Antennas; Morgan & Claypool: San Rafael, CA, USA, 2017; Volume 6, pp. 1–175.
60. Diaby, F.; Clemente, A.; Dussopt, L.; Sauleau, R.; Pham, K.; Fourn, E. Design of a 3-facet linearly-polarized transmitarray antenna at Ka-band. In Proceedings of the 2018 IEEE International Symposium on Antennas and Propagation & USNC/URSI National Radio Science Meeting, Boston, MA, USA, 8–13 July 2018; IEEE: Piscataway, NJ, USA, 2018.
61. Rana, B.; Lee, I.G.; Hong, I.P. Digitally reconfigurable transmitarray with beam-steering and polarization switching capabilities. IEEE Access 2021, 9, 144140–144148.
62. Pozar, D.M.; Targonski, S.D.; Syrigos, H. Design of millimeter wave microstrip reflectarrays. IEEE Trans. Antennas Propag. 1997, 45, 287–296.
63. Niu, T.; Withayachumnankul, W.; Ung, B.; Menekse, H.; Bhaskaran, M.; Sriram, S.; Fumeaux, C. Experimental demonstration of reflectarray antennas at terahertz frequencies. Opt. Express 2013, 21, 2875–2889.
64. Adamidis, G.; Vardiambasis, I. Design and Implementation of a 4 × 4 Butler-Matrix Switched-Beam Antenna Array at the Microwave Communications and Electromagnetic Applications Lab of

the Technological Educational Institute of Crete. In Proceedings of the 2005 WSEAS International Conference on Engineering Education (EE′05), Athens, Greece, 8–10 July 2005; pp. 374–379.

65. Adamidis, G.; Vardiambasis, I. Smart antenna design and implementation: A simple switched-beam antenna array based on a 8 × 8 Butler-matrix network. In Proceedings of the 10th WSEAS International Conference on Communications, Athens, Greece, 13–15 July 2006; WSEAS: Stevens Point, WI, USA, 2006.
66. Adamidis, G.A.; Vardiambasis, I.O.; Ioannidou, M.P.; Kapetanakis, T.N. Design and implementation of single-layer 4 × 4 and 8 × 8 Butler matrices for multibeam antenna arrays. Int. J. Antennas Propag. 2019, 2019, 1645281.
67. Capolino, F. Applications of Metamaterials; CRC Press: Boca Raton, FL, USA, 2017.
68. Balanis, C.A. Advanced Engineering Electromagnetics; John Wiley & Sons: Hoboken, NJ, USA, 2012.
69. Munk, B.A. Frequency Selective Surfaces: Theory and Design; John Wiley & Sons: Hoboken, NJ, USA, 2005.
70. Sarabandi, K.; Behdad, N. A frequency selective surface with miniaturized elements. IEEE Trans. Antennas Propag. 2007, 55, 1239–1245.
71. Li, M.N.B. Wideband true-time-delay microwave lenses based on metallo-dielectric and all-dielectric lowpass frequency selective surfaces. IEEE Trans. Antennas Propag. 2013, 61, 4109–4119.
72. Warren Stutzman, L.; Thiele, G.A. Antenna Theory and Design; John Wiley & Sons: Hoboken, NJ, USA, 2012.
73. Clemente, A.; Diaby, F.; Di Palma, L.; Dussopt, L.; Sauleau, R. Experimental validation of a 2-bit reconfigurable unit-cell for transmitarrays at Ka-band. IEEE Access 2020, 8, 114991–114997.
74. Di Palma, L.A.C.; Dussopt, L.; Sauleau, R.; Potier, P.; Pouliguen, P. Circularly-polarized reconfigurable transmitarray in Ka-band with beam scanning and polarization switching capabilities. IEEE Trans. Antennas Propag. 2017, 65, 529–540.
75. Diaby, F.; Clemente, A.; Sauleau, R.; Pham, K.T.; Dussopt, L. 2 Bit Reconfigurable Unit-Cell and Electronically Steerable Transmitarray at Ka-Band. IEEE Trans. Antennas Propag. 2019, 68, 5003–5008.
76. Xiao, Y.; Yang, F.; Xu, S.; Li, M.; Zhu, K.; Sun, H. Design and Implementation of a Wideband 1-Bit Transmitarray Based on a Yagi–Vivaldi Unit Cell. IEEE Trans. Antennas Propag. 2021, 69, 4229–4234.
77. Xiao, Y.; Xi, B.; Xiang, M.; Yang, F.; Chen, Z. 1-Bit Wideband Reconfigurable Transmitarray Unit Cell Based on PIN Diodes in Ku-Band. IEEE Antennas Wirel. Propag. Lett. 2021, 20, 1908–1912.

78. Wang, Y.; Xu, S.; Yang, F.; Werner, D.H. 1 Bit Dual-Linear Polarized Reconfigurable Transmitarray Antenna Using Asymmetric Dipole Elements with Parasitic Bypass Dipoles. IEEE Trans. Antennas Propag. 2020, 69, 1188–1192.
79. Wang, M.; Mo, Y.; Chen, Z.; Shan, K.; Liu, Z.; Feng, J.; Liu, Q.; Li, J. Design of A 4 × 4-Element High-Integrated Planar Pattern Reconfigurable Array Antenna. In Proceedings of the 2021 15th European Conference on Antennas and Propagation (EuCAP), Online, 22–26 March 2021; IEEE: Piscataway, NJ, USA, 2021.
80. Kozlov, D.; Munina, I.; Turalchuk, P.; Kirillov, V.; Shitvov, A.; Zelenchuk, D. Characterization of Tiled Architecture for C-Band 1-Bit Beam-Steering Transmitarray. Sensors 2021, 21, 1259.
81. Wang, M.; Xu, S.; Yang, F.; Li, M. Design and Measurement of a 1-bit Reconfigurable Transmitarray With Subwavelength H-Shaped Coupling Slot Elements. IEEE Trans. Antennas Propag. 2019, 67, 3500–3504.
82. Wang, M.; Xu, S.; Yang, F.; Hu, N.; Xie, W.; Chen, Z. A Novel 1-Bit Reconfigurable Transmitarray Antenna Using a C-Shaped Probe-Fed Patch Element with Broadened Bandwidth and Enhanced Efficiency. IEEE Access 2020, 8, 120124–120133.
83. Luo, C.-W.; Zhao, G.; Jiao, Y.-C.; Chen, G.-T.; Yan, Y.-D. Wideband 1 bit Reconfigurable Transmitarray Antenna Based on Polarization Rotation Element. IEEE Antennas Wirel. Propag. Lett. 2021, 20, 798–802.
84. Zhai, Z.; Zhao, G.; Sun, H. Design of a Wideband 1-bit 10 × 10 Reconfigurable Transmitarray in Ku Band. In Proceedings of the 2020 International Conference on Microwave and Millimeter Wave Technology (ICMMT), Shanghai, China, 20–23 September 2020; IEEE: Piscataway, NJ, USA, 2020.
85. Turalchuk, P.; Munina, I.; Kirillov, V.; Verevkin, A.; Zelenchuk, D. A C-band Transmitarray for Spatial Multiplexing and Diversity Applications. In Proceedings of the 2020 50th European Microwave Conference (EuMC), Utrecht, The Netherlands, 12–14 January 2021.
86. Munina, I.; Turalchuk, P.; Verevkin, A.; Kirillov, V.; Zelenchuk, D.; Shitvov, A. A study of C-band 1-bit reconfigurable dual-polarized transmitarray. In Proceedings of the 2019 13th European Conference on Antennas and Propagation (EuCAP), Krakow, Poland, 31 March–5 April 2019; IEEE: Piscataway, NJ, USA, 2019.
87. Lau, J.Y.; Hum, S.V. Analysis and characterization of a multipole reconfigurable transmitarray element. IEEE Trans. Antennas Propag. 2010, 59, 70–79.
88. Rotshild, D.; Rahamim, E.; Abramovich, A. Innovative Reconfigurable Metasurface 2-D Beam-Steerable Reflector for 5G Wireless Communication. Electronics 2020, 9, 1191.
89. Sun, Y.; Li, Z.; Zhu, W.; Ji, Z.; Wang, Q. New steerable antenna with controllable metamaterial. In Proceedings of the 2012 9th European Radar Conference, Amsterdam, The Netherlands, 31

October–2 November 2012; IEEE: Piscataway, NJ, USA, 2012.

90. Jiang, T.; Wang, Z.; Li, D.; Pan, J.; Zhang, B.; Huangfu, J.; Salamin, Y.; Li, C.; Ran, L. Low-DC voltage-controlled steering-antenna radome utilizing tunable active metamaterial. IEEE Trans. Microw. Theory Tech. 2011, 60, 170–178.
91. Russo, I.; Gaetano, D.; Boccia, L.; Amendola, G.; Di Massa, G. Investigation on the transmission beam-steering capabilities of tunable impedance surfaces. In Proceedings of the 2009 European Microwave Conference (EuMC), Rome, Italy, 29 September–1 October 2009; IEEE: Piscataway, NJ, USA, 2009.
92. Padilla, P.; Muñoz-Acevedo, A.; Castañer, M.S.; Sierra-Pérez, M. Electronically Reconfigurable Transmitarray at Ku Band for Microwave Applications. IEEE Trans. Antennas Propag. 2010, 58, 2571–2579.
93. Frank, M.; Lurz, F.; Weigel, R.; Koelpin, A. Electronically reconfigurable 6 × 6 element transmitarray at K-band based on unit cells with continuous phase range. IEEE Antennas Wirel. Propag. Lett. 2019, 18, 796–800.
94. Tang, J.; Xu, S.; Yang, F.; Li, M. Design and Measurement of a Reconfigurable Transmitarray Antenna with Compact Varactor-based Phase Shifters. IEEE Antennas Wirel. Propag. Lett. 2021, 20, 1998–2002.
95. Reis, J.R.; Caldeirinha, R.F.S.; Hammoudeh, A.; Copner, N. Electronically reconfigurable FSS-inspired transmitarray for 2-D beamsteering. IEEE Trans. Antennas Propag. 2017, 65, 4880–4885.
96. Nicholls, J.G.; Hum, S.V. Full-space electronic beam-steering transmitarray. IEEE Trans. Antennas Propag. 2016, 64, 3410–3422.
97. Frank, M.; Weigel, R.; Koelpin, A. Design of a 24 GHz reconfigurable transmitarray element with continuous phase range. In Proceedings of the 2017 11th European Conference on Antennas and Propagation (EUCAP), Paris, France, 19–24 March 2017; IEEE: Piscataway, NJ, USA, 2017.
98. Reis, J.R.; Vala, M.; Oliveira, T.E.; Fernandes, T.R.; Caldeirinha, R.F.S. Metamaterial-Inspired Flat Beamsteering Antenna for 5G Base Stations at 3.6 GHz. Sensors 2021, 21, 8116.